The 6th ASME-JSME Thermal Engineering Joint Conference
March 16-20, 2003

TED-AJ03-275

A MOLECULAR DYNAMICS SIMULATION OF FORMATION PROCESS OF SWNTS IN CCVD METHOD

Yasushi SHIBUTA
Department of Mechanical Engineering,
The University of Tokyo
7-3-1 Hongo, Bunkyo-ku, Tokyo, 113-8656, Japan
E-mail: shibuta@photon.t.u-tokyo.ac.jp

Shigeo MARUYAMA
Department of Mechanical Engineering,
The University of Tokyo
7-3-1 Hongo, Bunkyo-ku, Tokyo, 113-8656, Japan
E-mail: maruyama@photon.t.u-tokyo.ac.jp

Keywords: Molecular Dynamics Method, Carbon Nanotube, Catalytic Chemical Vapor Deposition, Formation Mechanism, Catalytic Metal

ABSTRACT

Developments of large scale and high-purity generation technique of single-walled carbon nanotubes (SWNTs) [1] are desired for the practical applications of the fascinating new material. In addition to previously known laser-furnace [2] and arc-discharge [3] techniques, recently, the catalytic chemical vapor deposition (CCVD) method [4] has been developed for the possible larger amount production with lower cost. We have developed a high-quality production technique of SWNTs at low-temperature by using alcohol as carbon source [5]. For the better control of the generation process, understanding of the formation mechanism is inevitable. We had constructed the classical potential function between carbon clusters and several metal atoms (La, Sc and Ni) based on DFT calculations of small metal-carbon binary clusters for the simulation of the formation process of the endohedral metallofullerene [6].

At first, with the same potential for carbon and Ni, we have explored the formation process of SWNTs in the laser-furnace technique. Starting from randomly distributed carbon and Ni atoms, random cage structures of carbon atoms with a few Ni atoms were obtained after 6 ns simulation. Ni atoms on the random cage prohibited the complete closure and anneal of the cage structure into the fullerene structure. Collisions of such imperfect random-cage clusters lead to an elongated tubular cage structure [7].

However, the formation mechanism in CCVD method should be considerably different from the laser-furnace case, because the catalytic metal clusters or particles are present before the assembly of carbon atoms. Carbon atoms should arrive as units of a few atoms determined by the carbon source molecule. In the next stage, we performed the molecular dynamics simulation of formation process of SWNTs in CCVD method. Starting from randomly distributed carbon atoms and a Ni cluster, the clustering process to a SWNT was simulated. Since the carbon source such as methane and ethanol decomposed to solid carbon only at the catalytic metal surface, specially designed van der Waals potential in the simulation prohibited clustering of carbon-carbon atoms, even though hydrogen or oxygen atoms were not explicitly included. Depending on the initial Ni cluster size and on temperature, the formation of various nanotube cap structures was demonstrated. The cap on the Ni_{108} cluster grew up to the tubular structure at 2500K as in Figure A-1.

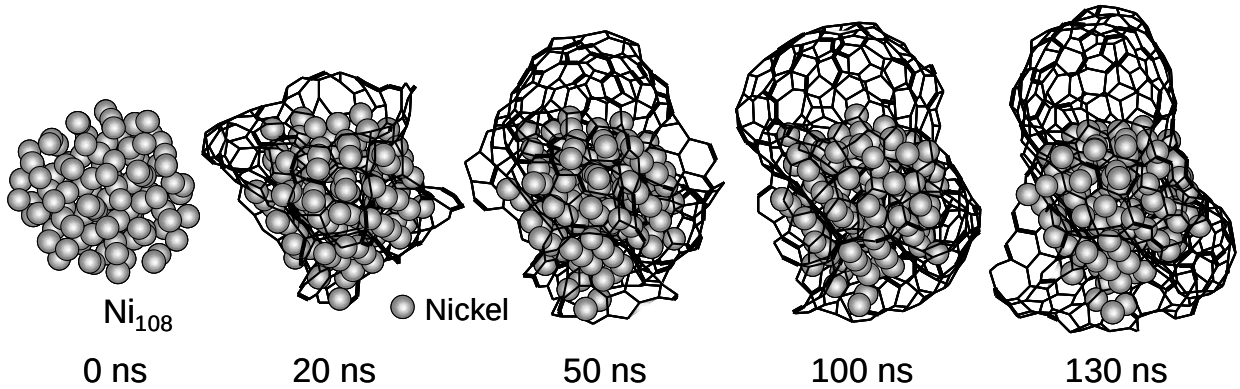

Figure A-1. Snapshots of metal-catalyzed growth of the cap-structure at 2500K.
Gray circles represent nickel atoms. All carbon atoms are not shown for clarity.

INTRODUCTION

Discoveries of multi-walled carbon nanotubes (MWNTs) [8] and single walled carbon nanotubes (SWNTs) [1] have opened new research and application fields with the carbon material. Even though the macroscopic generation of SWNTs with the laser-furnace technique [2], the arc-discharge technique [3], and the catalytic chemical vapor deposition (CCVD) technique [4,5] has been demonstrated, the formation mechanism of SWNTs is still not clear. Besides the theoretical interest of the self-assembly formation of such elongated perfect structure of carbon, understandings of the formation mechanism are crucial for the development of purer and larger amount and hopefully chirality-controlled generation technique of SWNTs.

Theoretical contributions to the formation mechanism of carbon nanotubes were limited since the system size and time scales were far beyond the simple simulation of the whole process. Several previous classical molecular dynamics calculations [9, 10] examined the specific points of generation mechanism with Brenner potential [11] for pure carbon system. Hence the roles of metal catalysis were not fully discussed. It was because a reliable classical potential function between metal and carbon was not known. We had constructed the classical potential function between carbon clusters and several metal atoms (La, Sc and Ni) based on DFT calculations of small metal-carbon binary clusters for the simulation of the formation process of the endohedral metallofullerene [6]. Using these potential functions, molecular dynamics simulations of formation process in the laser-furnace method and in the CCVD method were studied.

The formation mechanism in CCVD method and in the laser-furnace method should be considerably different. In the former method, the catalytic metal clusters are present before the assembly of carbon atoms. In the latter, carbon atoms and catalytic metal atoms are vaporized at the same time by the intense laser ablation. The growth process in CCVD method is regarded as the heterogeneous nucleation in contrast to the, in a sense, homogeneous nucleation in the laser-furnace method. Both situations are compared with molecular dynamics simulations. For laser-furnace process, from randomly distributed metal and carbon atoms, imperfect cage clusters with a metal atom prohibiting the closure were obtained. Collisions of these clusters lead to the imperfect SWNT structure. On the other hand, for CCVD process, depending on the initial Ni cluster size and on temperature, the formation of various nanotube cap structures was demonstrated. Based on these results, the critical formation mechanism and diameter selection of SWNTs are discussed.

NOMENCLATURE

B^* = valence function
b = potential parameter
c = number of charges
D_e = depth of potential
E_b = binging energy
f = cut-off function
R_e = interatomic distance of equilibrium
r_{ij} = distance between atom i and j
S = potential paramater
T_c = control temperature
t = time
V_A = attractive term
V_R = repulsive term
β = potential parameter
δ = potential parameter
C = carbon atom
M = metal atom

SIMULATION TECHNIQUE

Carbon-carbon potential for covalent bonding

We employed the Brenner potential [11] for carbon-carbon covalent bonding. This potential could describe variety of small hydrocarbons and graphite and diamond lattices. The basic formulation of the potential was based on the covalent-bonding treatment developed by Tersoff [12]. The total potential energy of the system E_b was expressed as the sum of the bonding energy of each bond between carbon atoms i and j.

$$E_b = \sum_i \sum_{j(i<j)} \left[V_R(r_{ij}) - B_{ij}^* V_A(r_{ij}) \right], \tag{1}$$

where $V_R(r)$ and $V_A(r)$ were repulsive and attractive force terms, respectively. The Morse type form with a cut-off function $f(r)$ expressed these terms.

$$V_R = f(r) \frac{D_e}{S-1} \exp\left\{ -\beta\sqrt{2S}(r - R_e) \right\} \tag{2}$$

$$V_A = f(r) \frac{D_e S}{S-1} \exp\left\{ -\beta\sqrt{2/S}(r - R_e) \right\} \tag{3}$$

$$f(r) = \begin{cases} 1 & (r < R_1) \\ \frac{1}{2}\left(1 + \cos\frac{r - R_1}{R_2 - R_1}\pi \right) & (R_1 < r < R_2) \\ 0 & (r > R_2) \end{cases} \tag{4}$$

The effect of the bonding condition of each atoms was taken into account through B^*_{ij} term which was the function of angle θ_{ijk} between bonds i-j and i-k.

$$B_{ij}^* = \frac{B_{ij} + B_{ji}}{2}, B_{ij} = \left(1 + \sum_{k(\neq i,j)} G_c(\theta_{ijk}) f(r_{ik}) \right)^{-\delta}, \tag{5}$$

where

$$G_c(\theta) = a_o \left(1 + \frac{c_o^2}{d_o^2} - \frac{c_o^2}{d_o^2 + (1 + \cos\theta)^2} \right). \tag{6}$$

Constants were as fellows:

D_e = 6.325 eV S = 1.29 β = 1.5 Å^{-1}
R_e = 1.315 Å δ = 0.80469
a_0 = 0.011304 c_0 = 19 d_0 = 2.5
R_1 = 1.7 Å R_2 = 2.0 Å.

Here, we have ignored [13] the term for the conjugate bond from original expressions of Brenner.

Carbon-metal and metal-metal potential

We had constructed the classical potential function between carbon clusters and several metal atoms (La, Sc

and Ni) based on DFT calculations of small metal-carbon binary clusters for the simulation of the formation process of the endohedral metallofullerene [6]. Here, we employed this potential for the Ni-carbon and Ni-Ni interaction.

Ni-carbon multi-body potential were constructed as functions of the carbon coordinate number of a metal atom. The coordinate number of the metal atom N^C is defined using the cutoff function $f(r)$, and the additional term B^* was expressed as the function of the coordinate number. Here, the effect of the angle among bonds is ignored.

$$N^C = 1 + \sum_{carbon k(\neq j)} f(r_{ik}) \tag{7}$$

$$B^* = \left\{1 + b(N^C - 1)\right\}^{\delta} \tag{8}$$

For metal-metal interactions, we expressed the equilibrium binding energy D_e and the bond length R_e as direct function of the metal coordinate number N_{ij}, instead of using the additional term B^*.

$$N_i^M = 1 + \sum_{metal\ k(\neq j)} f(r_{ik}), \quad N_{ij} = \frac{N_i^M + N_j^M}{2} \tag{9}$$

$$D_e(N_{ij}) = D_{e1} + D_{e2} \exp\left\{-C_D(N_{ij} - 1)\right\} \tag{10}$$

$$R_e(N_{ij}) = R_{e1} - R_{e2} \exp\left\{-C_R(N_{ij} - 1)\right\} \tag{11}$$

Constants for Ni-carbon were as follows:

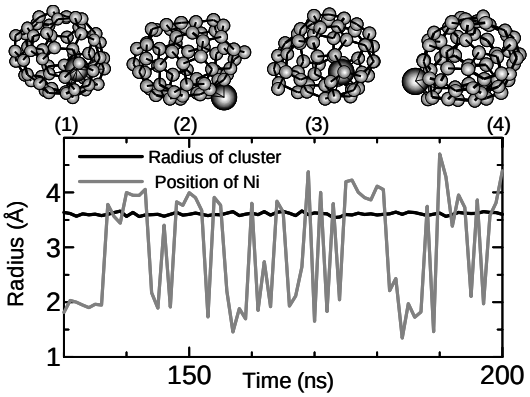

Figure 1. Annealing of NiC_{60}.

D_e = 3.02 eV S = 1.3 β = 1.8 Å^{-1}
R_e = 1.7 Å δ = -0.8 b = 0.0330
R_1 = 2.7 Å R_2 = 3.0 Å.

And constants for Ni-Ni were as follows:

S = 1.3 β = 1.55 Å^{-1}
D_{e1} = 0.74 Å D_{e2} = 1.423
R_{e1} = 2.520 Å R_{e2} = 0.304 Å
C_D = 0.365 C_R = 0.200
R_1 = 2.7 Å R_2 = 3.2 Å.

Van der Waals potential for CCVD method

Assuming that the carbon source such as methane and ethanol decomposed to the solid carbon molecule only at the catalytic metal surface in CCVD method, we employed the van der Waals potential between molecules to prohibit the clustering. Here we did not include hydrogen or oxygen in the simulation, but simply carbon atoms with the van der Waals potential represented the carbon source molecules in gas-phase. Since we did not assume the van der Waals potential between Ni and carbon atoms, carbon molecules could easily attach to Ni cluster. The immediate decomposition of the carbon source molecules leaving a carbon atom was assumed. As soon as a carbon attached to the Ni cluster, van der Waals potential between carbon atoms was removed. As for the van der Waals potential,

$$E_{LJ} = 4\varepsilon\left(\left(\frac{\sigma}{r_{ij}}\right)^{12} - \left(\frac{\sigma}{r_{ij}}\right)^{6}\right) \tag{12}$$

with the parameters known for carbon-carbon interaction as

ε = 2.4 meV, σ = 3.37 Å.

Integration of the equation of motion

Velocity Verlet method was employed to integrate the classical equation of motion with the time step of 0.5 fs. All calculations were performed in a cubic box with periodic boundary conditions in all 3 directions. When temperature control was enforced, the simple velocity scaling was adopted.

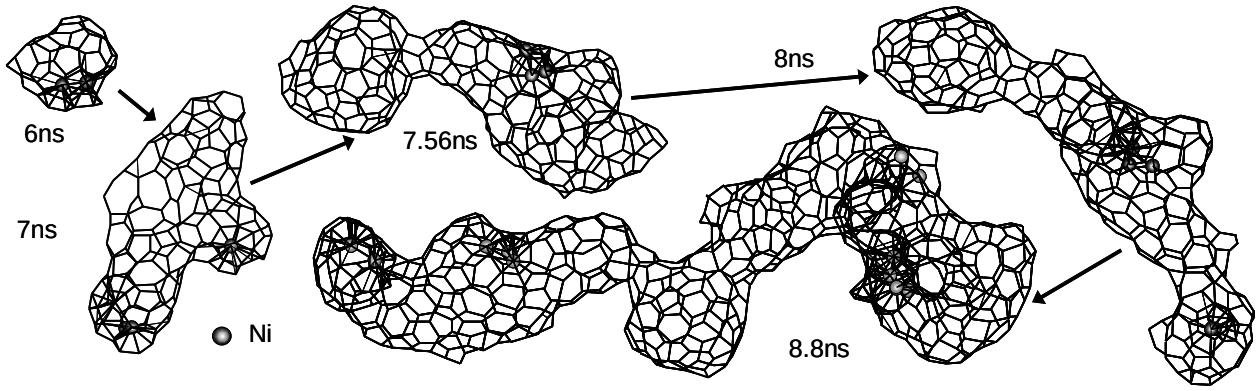

Figure 2. Growth process of a tubular structure by successive collisions of imperfect cage cluster. (All carbon atoms with three-coordination are not shown.)

RESULTS AND DISCUSSIONS

Simulations for laser-furnace technique

In the laser-furnace method, carbon atoms and catalytic metal atoms are vaporized at the same time by the laser ablation. As for the initial condition, the completely random vapor mixture of 2500 carbon atoms and 25 Ni atoms was allocated in 585 Å cubic fully-periodic simulation cell. The high density of the system was compensated with the very rapid cooing with the temperature control. Through this rapid temperature control, energy distribution between translation, rotation, and vibration may be unrealistically in non-equilibrium. Hence, the special temperature control method that control translational, rotational and vibrational temperature of the system independently was employed. The control temperature was set to 3000 K. Many relatively large clusters up to about 200 carbon atoms with a few Ni atoms were obtained after 6 ns simulation. Carbon clusters tended to be spherical random cage structure with a few metal atoms at around the defect vacancy, which prevented the cage structure from the complete closure [7].

As in our empty fullerene and metallofullerene studies, these cluster structures were not well annealed because of the accelerated simulations. An example of the annealing simulation of the Ni-attached carbon cluster is shown in Fig. 1. Picking up a NiC_{60} cluster in the simulation cell, vibrational annealing process was simulated for 200 ns without additional collisions at 2500K. As clearly seen in Fig. 1, quasi-periodic motion of the Ni atom flipping inside and outside of the carbon cage was observed. The possibility of this meta-stable structure should be confirmed with more accurate *ab initio* level calculations. These imperfect carbon cage structures with several metal atoms outside were partially confirmed by the FT-ICR [14] reaction experiments of laser vaporized clusters [15].

In the real generation situation of SWNTs, it is expected that those clusters experience later collisions at lower temperature and lower frequency as they expand. However, because of the computational limitations, we had to slowly shrink the simulation cell to enhance the collisions. The shrinking rate was set as 6×10^{-5} Å per time step (about 12 m/s), which was much slower than the typical translational velocity of clusters. The large particle with some tubular structure was obtained after collisions of clusters.

Figure 2 shows the growth process of the typical tubular cluster from shrinking simulation at 2000K. Again, in order to accelerate the simulation of annealing, we applied higher temperature than the typical experimental condition. Even though the structure shown in Fig. 2 is rather ugly, one can see that the tubular structure has grown longer by collisions and the coalescences. Ni atoms were slowly assembling to form Ni clusters, and they were diffusing around until finding the most stable position at the hemi-half-fullerene cap area.

Part of the anneal tendency was examined by separate simulations as shown in Fig. 3. An intermediate structure appeared in Fig. 2 (8 ns) was picked up for this annealing. Comparison of annealing effect with different temperatures (2000K and 2500K) for 50 ns is shown in Figure 3. The tubular structure became thick at the narrow part and almost straight due to the annealing. And, the clustering of Ni atoms was observed for 2500K case. The metal cluster tended to stick to the curved carbon structure. Unfortunately, in the case of Fig. 3, the metal cluster was trapped in the curved defect part in the middle of the tubular structure. Since the narrow part of the tubular structure was usually Ni free, the tubular structure can be annealed to SWNT structure.

From these simulations, the catalytic effect of Ni atoms in laser-furnace method may be explained as follows. At the clustering stage, Ni atoms tend to stay at around the defect vacancy of carbon cage structure, and prevent the cage from closing to fullerene. Then, the random cage carbon clusters can make further growth by colliding with each other at the large defect area of the cage. The collision leads to the elongated tubular structure as shown in Fig. 2. Given the enough time for diffusion of metal atoms and network annealing, we expect that the structure becomes a straight SWNT with metal cluster at each end.

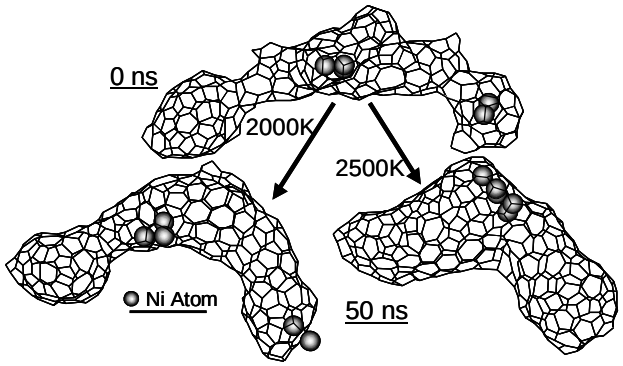

Figure 3. Annealing at 2000K and 2500K of intermediate structure.

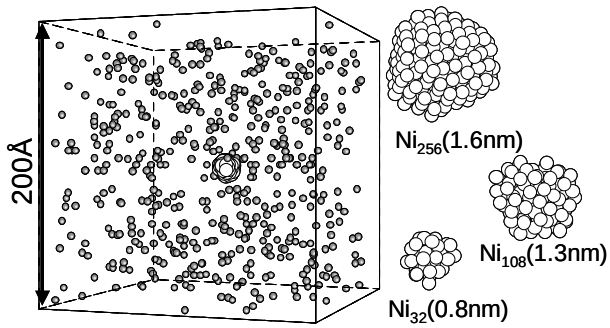

Figure 4. Initial condition of clustering process in CCVD method.

Simulations for CCVD method

In the CCVD method, the catalytic metal clusters are present before the assembly of carbon atoms. At first, we obtained the initial Ni cluster structures of various sizes by annealing FCC crystal structure at 2 ns in 2000K. As the initial condition of clustering process, the completely random vapor mixture of 500 carbon atoms and one of the Ni clusters obtained above were allocated in 200 Å cubic fully-periodic simulation cell. Figure 4 shows an example of the initial configuration. In this case, interaction between isolated carbons was represented by the Lennard-Jones potential described in Eq. (12). Simulation results are shown in Fig. 5 as snapshots. Carbon atoms covered the surface of the Ni cluster one step at a time at 2500K. At 8 ns, almost whole surface of catalytic metal was covered by the graphitic structure. On the other hand, amorphous-like carbon attached to the surface of the catalytic metals at lower temperature, 1000K. Neither condition lead to the elongated structure at this stage.

Here, we noticed the problem in our algorithm of the carbon decomposition process. Since we turned off the Lennard-Jones interaction between carbon and carbon, when one of the carbons belonged to the metal-carbon cluster, a carbon atom (which is really a hydro-carbon molecule) can attach to the carbon structure well outside of the catalytic metal cluster. Since we believed that the carbon source molecule such as methane and ethanol decomposed to solid carbon only at the catalytic metal surface, we had to avoid the easy bonding between the isolated carbon (carbon source molecules) and the carbon on the metal surface in order to describe the decomposition on the catalytic metal.

In the next simulations, all interactions between carbon-carbon were included with the Lennard-Jones potential described in Eq. (12). In this case, carbon atoms can make covalent bonding each other only when both atoms were attaching to the surface of catalytic metals. The initial condition of clustering process was the same as the former simulation. Carbon atoms attached to the exposed surface of catalytic metal and diffused on the surface to make covalent bond with other carbon atoms. Figure 6 shows the aggregation of carbon atoms on Ni clusters observed for various conditions. Carbon atoms attached on the exposed surface and some of them precipitated from another face of the particles step by step. Figure A-1 shows an example of this process on the Ni_{108} at 2500K. The precipitated carbon atoms had graphitic structure, and further sequence of attaching and precipitating from the sphere side of the metal cluster led to the cap structure. On the other hand, carbon atoms moved less actively to precipitate as the graphitic structure at 1500K. In that temperature, carbon atoms and metal atoms wouldn't dissolve well in this simulation. This tendency was in good agreement with the phase diagrams from experimental data [16].

CONCLUSIONS

From molecular dynamics simulations, the catalytic effect of metal atoms may be explained as follows. In the laser-furnace method, Ni atoms tend to stay at around the defect vacancy of carbon cage structure, and prevent the cage from closing to fullerene. Then, the random cage carbon clusters can make further growth by colliding with each other at the large defect area of the cage. The collision leads to the elongated tubular structure. Given the enough time for diffusion of metal atoms and network annealing, we expect that the structure becomes a straight SWNT with metal clusters at each end. On the other hand, in the CCVD method, carbon atoms chemisorpted on the exposed surface of catalytic metal, diffused near the surface and moved to make covalent bond with other carbon atoms. As increasing the number of carbon atoms, some of them precipitated to be elevated from the surface. Further simulation may lead to the cap structure that is regarded as the nucleus of SWNTs.

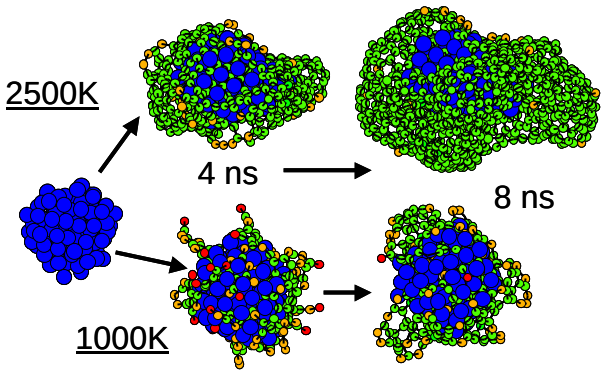

Figure 5. Snapshots of aggregation of carbon atoms on Ni_{108} particles. Blue atoms show the nickel atoms. Green, orange and red spheres represent the carbon atoms, which have three, two, one covalent bond, respectively.

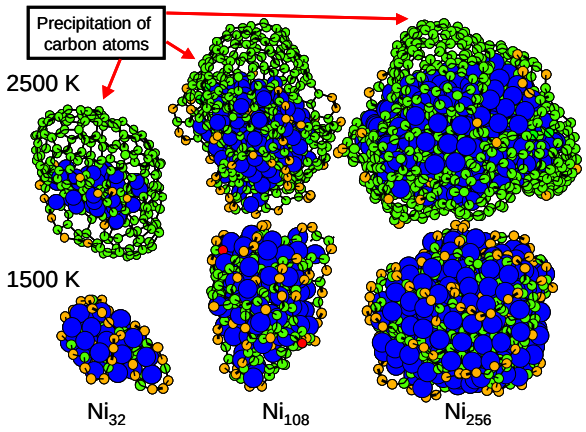

Figure 6. Snapshots of aggregation of carbon atoms on a nickel cluster at 50 ns. Blue atoms show the nickel atoms. Green, orange and red spheres represent the carbon atoms, which have three, two, one covalent bond, respectively.

ACKNOWLEDGMENT

The author would like to thank Dr. Yasutaka Yamaguchi (Osaka Univ.) for their help in molecular dynamics simulations. Part of this research was supported from Grant-in-aid for Scientific Research (#12450082, #13555050, #12GS0019).

REFERENCES

[1] Iijima, S. and Ichihashi, T., "Single-Shell Carbon Nanotubes of 1-nm Diameter", Nature, 363, (1993), 603-605.

[2] Thess, A., Lee, R., Nikolaev, P., Dai, H., Petit, P., Robert, J., Xu, C., Lee, Y.H., Kim, S.G., Rinzler, A.G., Colbert, D.T., Scuseria, G.E., Tománek, D., Fischer, J.E., Smalley, R.E., "Crystalline Ropes of Metallic Carbon Nanotubes" Science, 273, (1996), 483-487.

[3] Journet, C., Maser, W.K., Bernier, P., Loiseau, A., de la Chapelle, M.L., Lefrant, S., Deniard, P., Lee, R., Fisher, J.E., "Large-Scale Production of Single-Walled Carbon Nanotubes by the Electric-Arc Technique", Nature, 388, (1997), 756-758.

[4] Dai, H., Rinzler, A.G, Nikolaev, P., Thess, A., Colbert, D.T., Smalley, R.E., "Single-Wall Nanotubes Produced by Metal-Catalyzed Disproportionation of Carbon Monoxide", Chem. Phys. Lett., 260, (1996), 471-475.

[5] Maruyama, S., Kojima, R., Miyauchi, Y., Chiashi, S., and Kohno, M., "Low-Temperature Synthesis of High-Purity Single-Walled Carbon Nanotubes from Alcohol", Chem. Phys. Lett., 360, (2002), 229-234.

[6] Yamaguchi, Y. and Maruyama, S., "A Molecular Dynamics Study on the Formation of Metallofullerene", Euro. Phys. J. D., 9, (1999), 385-388.

[7] Shibuta, Y. and Maruyama, S., "Molecular Dynamics Simulation of Generation Process of SWNTs", Physica B, 323, (2002), 187-189.

[8] Iijima, S., "Helical Microtubules of Graphitic Carbon", Nature, 354, (1991), 56-58.

[9] Maiti, A., Brabec, C.J., Roland, C. and Bernholc, J., "Theory of Carbon Nanotube Growth", Phys. Rev. B, 52, (1995), 14850-14858.

[10] Maiti, A., Brabec, C.J. and Bernholc, J., "Kinetics of Metal-Catalyzed Growth of Single-Walled Carbon Nanotubes", Phys. Rev. B, 55, (1997), 6097-6100.

[11] Brenner, D.W., "Empirical Potential for Hydrocarbons for Use in Simulating the Chemical Vapor Deposition of Diamond Films", Phys. Rev. B., 42, (1990), 9458-9471.

[12] Tersoff, J., "New Emperical Model for the Structural Properties of Silicon", Phys. Rev. Lett., 56, (1986), 632-635.

[13] Yamaguchi, Y. and Maruyama. S., "A Molecular Dynamics Simulation of the Fullerene Formation Process", Chem. Phys. Lett., 286, (1998), 336-342.

[14] Maruyama, S., Anderson, L.R. and Smalley, R.E., "Laser Annealing of Silicon Clusters", J. Chem., Phys., 93, (1990), 5349-5351.

[15] Maruyama, S., "Perspectives of Fullerene Nanotechnology", Dordrecht, Kluwer Academic Publishers, (2002).

[16] Thaddeus, B., Massalski, "Binary Alloy Phase Diagrams", Ohio, Metals Park: American Society for Metals, (1986).